A MULTI-PARAMETER STATISTICAL ANALYSIS OF THE CONNECTION BETWEEN H_2O MASER EMISSION AND NUCLEAR GALACTIC ACTIVITY

Emil Christensen (JMU), Anca Constantin (JMU) , Jim Braatz (NRAO-UVa), Robert Roten (JMU), Andrew Nutter (JMU)

Abstract

Water mega-maser disks currently provide the most accurate and direct method for calculating distances to galaxies and for weighing super massive black holes (SMBHs). Moreover, high spatial resolution radio mapping of these systems provide the most direct view of the process of accretion of matter onto SMBHs. It is thus of great importance to understand how the maser-emission and the masing conditions relate to their host properties, and in particular, with their nuclear nebular activity. We present here the results of a comprehensive multi-parameter analysis of high-quality photometric and spectroscopic measurements of the largest sample of galaxies surveyed for water maser emission. We use both individual parameter correlation analyses and a Principal Component Analysis to constrain the type and range of optical characteristics that best associate with various morphologies and strengths of water maser activity. We present these results in the frame of current proposed models of galactic evolution processes suggesting that the mega-maser phenomenon could be related to a certain brief phase in the active galactic nucleus life-time. This analysis provides new sophisticated yet feasible criteria for targeting these systems with a projected 4-fold increase in the detection rate.

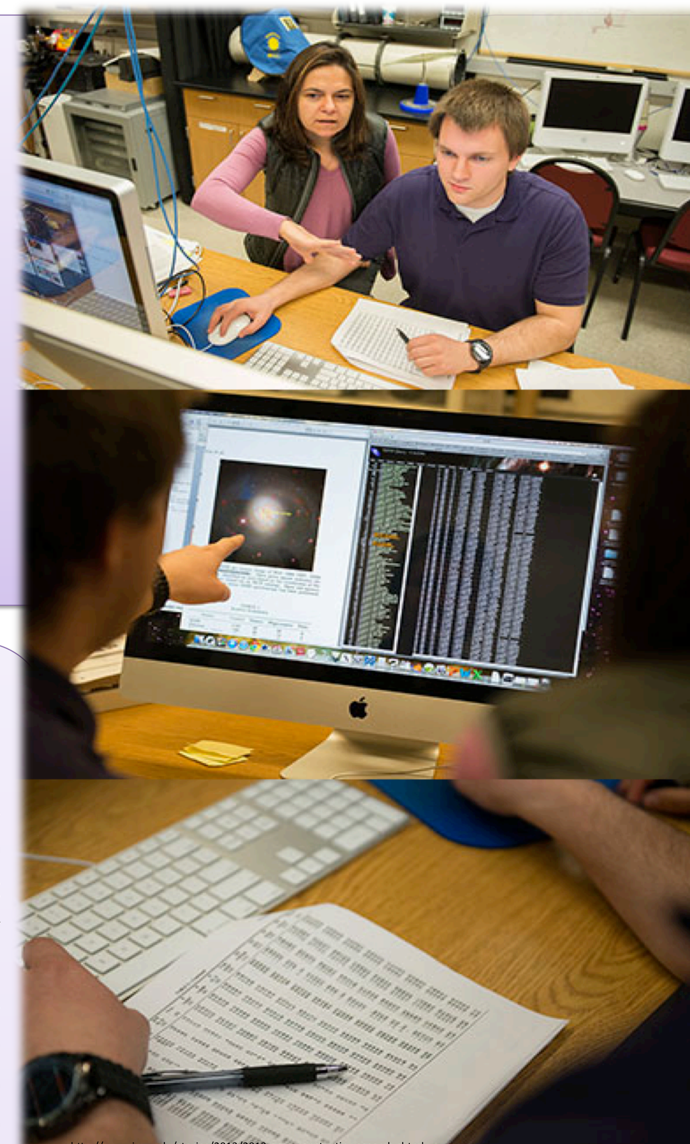

Data and Measurements

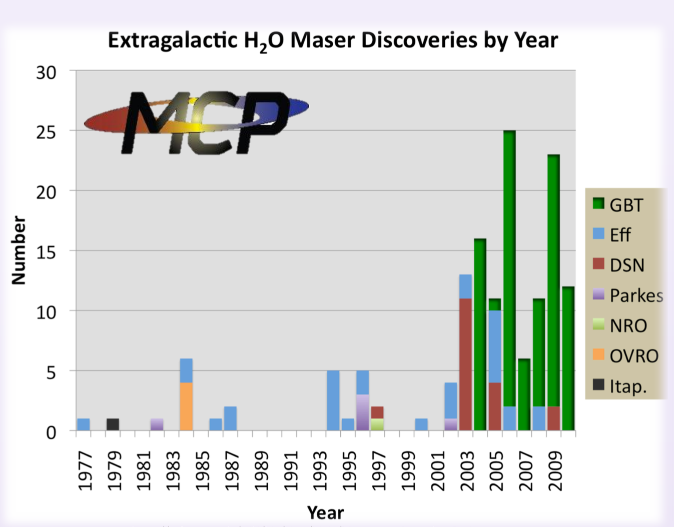

Mega-maser disks are sparse. The detection rate of maser emission in galactic nuclei is only ~4%. Out of ~3500 galaxies surveyed to date only 151 galaxies were found to host maser emission (The Megamaser Cosmology Project; MCP; e.g., Reid et al. 2009, 2013) . Only 34 (23%) of these appear to be mega-masers (L_{H2O} > 10 L_{sun}) with a disk like configuration. In an attempt to increase the efficiency in mega-maser detection in future surveys, we characterize and compare a wide variety of nuclear and host optical properties of galaxies with and without detected maser emission.

Cross Matching

The results of cross matching the MCP maser and non-maser samples with large optical spectroscopic surveys (Palomar; e.g., Ho et al. 2009, and references therein, and SDSS; Abazajian et al. 2009) are listed in the table below. We performed visual inspection of every match in order to assure that all matches were indeed nuclear. We present examples of good (nuclear) and bad (non-nuclear) matches to the right. For the maser galaxies that are not included in the Palomar or SDSS surveys, we searched the literature for spectral and photometric information.

Good Match (Nuclear) | Bad Match (non-nuclear)

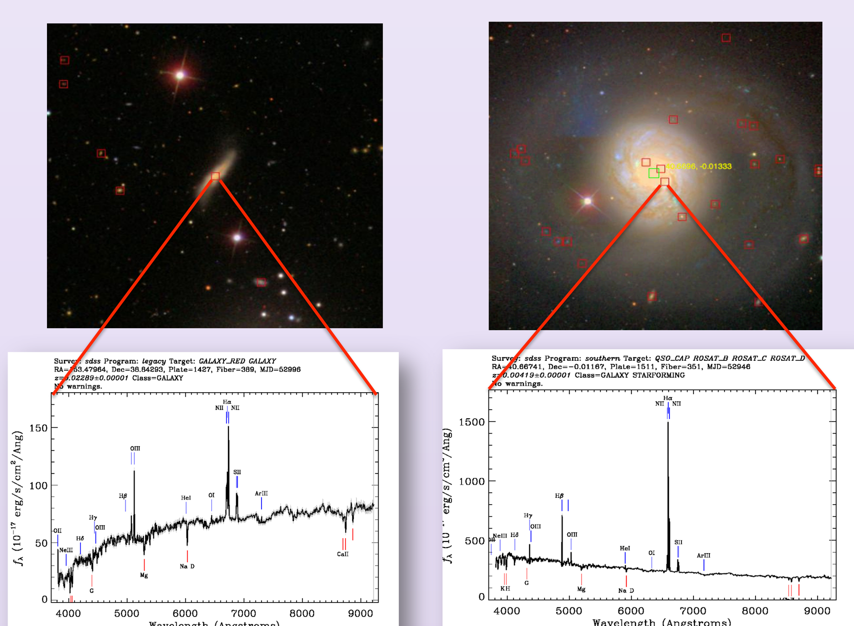

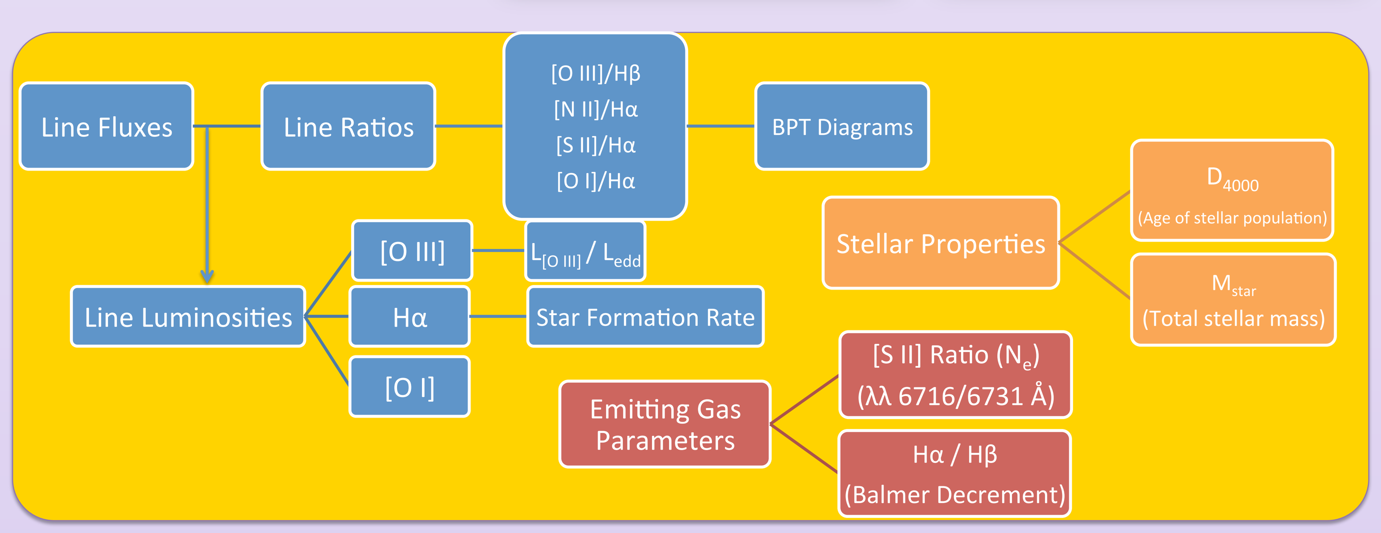

Measurements of the host and nuclear nebular emission of the SDSS galaxies are drawn from the MPA/JHU catalogue (Brinchmann et al. 2004). For all of the spectral measurements employed in this study, the emission-line component is measured after it is separated from the host stellar emission. Black Hole masses (M_{BH}) and corresponding accretion rates (measured via the Eddington ratio) are obtained based on estimates of the stellar velocity dispersion (σ*). For the SDSS objects only, we also relate the maser and the central BH accretion activity to the host properties by employing stellar masses and the D_n4000 break, as calculated and presented by Kauffman et al. (2003, 2004).

Source	Control	Masers	Mega-masers	Disks
SDSS	1181	46	34	7
Palomar	183	26	11	4
Palomar & SDSS[a]	25	7	2	1
Other[b]	0	27	22	5
Total	1339	92	65	15

[a] Galaxies with both Palomar and SDSS spectra; in these cases, we adopt the Palomar spectra and measurements.
[b] Bennert et al. (2004); Dahari & De Robertis (1988); Kim et al. (1995); Whittle (1992); Neugebauer et al. (1976); Adams & Weedman (1975); Phillips et al. (1983); Osterbrock & De Robertis (1985); Goodrich & Osterbrock (1983); De Robertis & Osterbrock (1986); Moustakas & Kennicutt (2006); Buttiglione et al. (2009)

Optical Spectral Types and Maser Activity

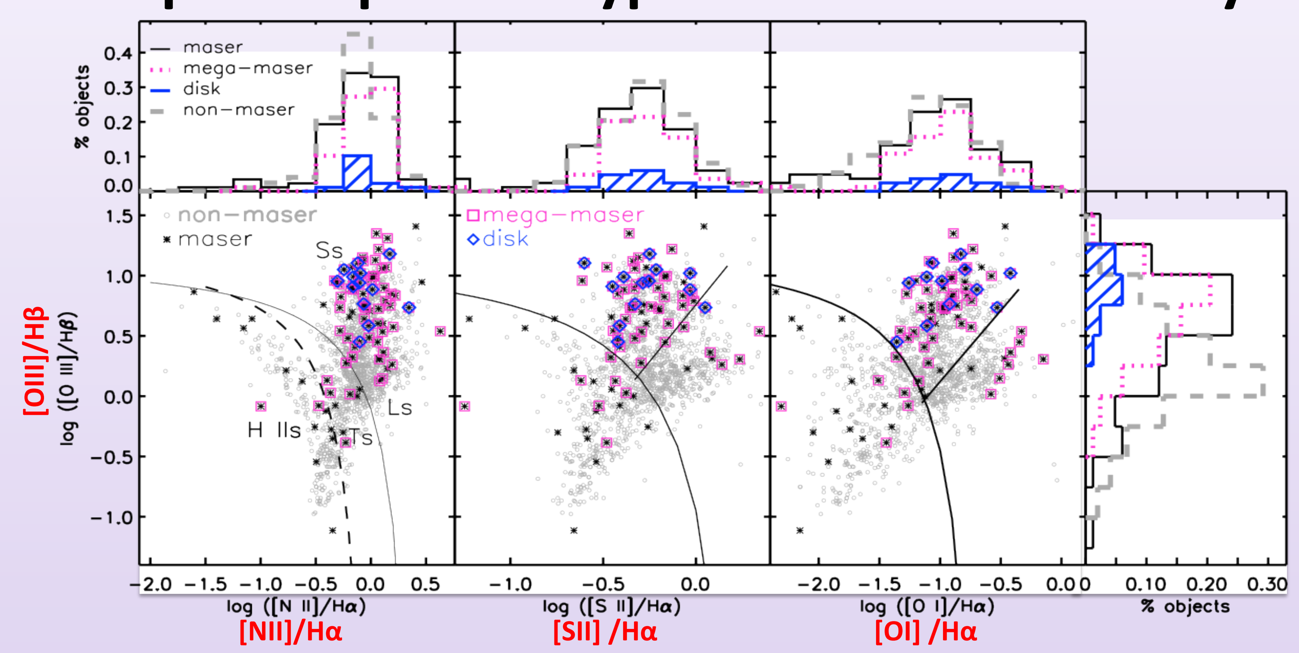

Line diagnostic diagrams are useful for identifying the dominant ionization mechanisms in galactic nuclei. Star forming galaxies (H II's), where ionization is produced by hot young stars, have low [O III], [N II], [S II] and [O I] emission while Seyferts show strong emissions in these features. Transition Objects (Ts) and the Low Ionization Nuclear Emission Regions (LINERs, Ls) show an intermediate behavior, and thus, probably a mix of these two ionization types. We adopt the criteria of Kewley et al. (2006). These diagrams reveal that **maser emission is not exclusively associated with Seyfert type activity as previously believed. The maser detection rate is clearly non-zero for non-accreting sources.** It is also apparent that maser galaxies tend to have a higher [O III]/Hβ flux ratios, a property that can be exploited in future survey target selection.

The characteristics that differentiate between masers and non-masers

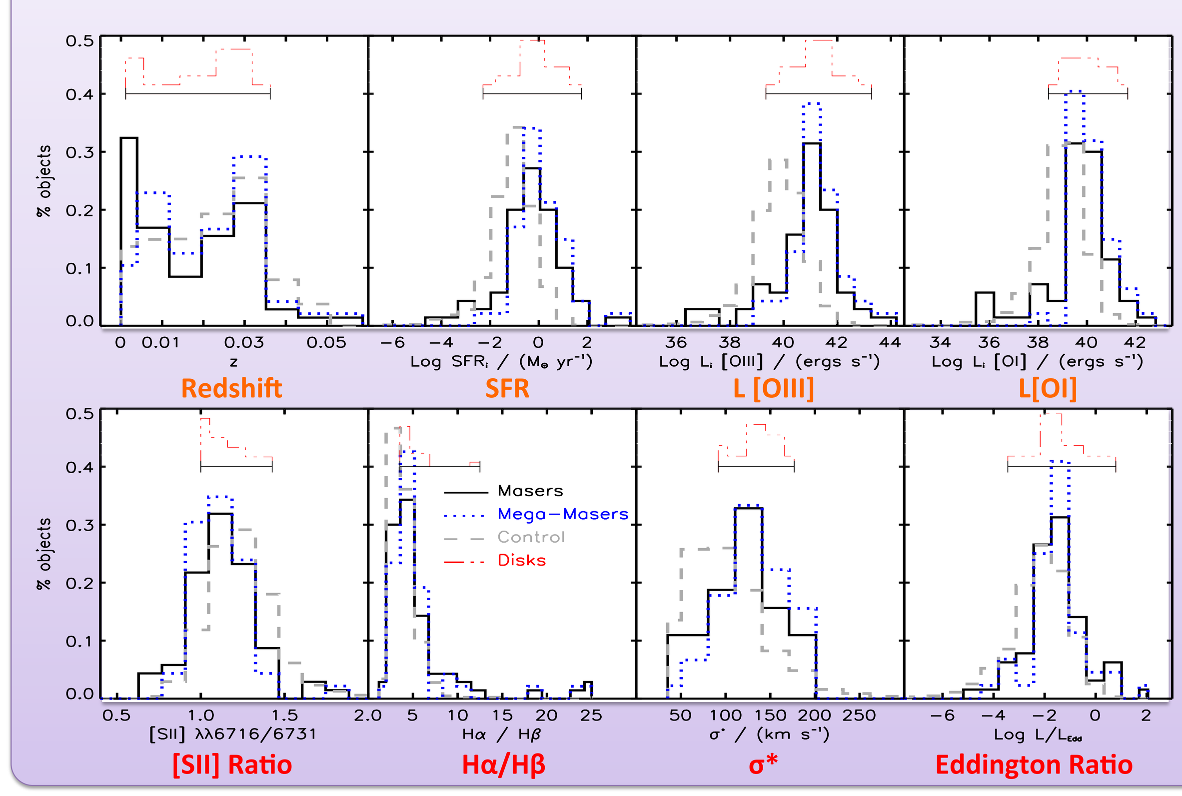

Kolmogorov-Smirnov (K-S) Statistics

The K-S statistic is a method of quantifying the probability that two distributions share the same parent population. K-S probabilities are consistently low for the control/mega-maser comparison, showing that they do not share the same parent set of characteristics, even if they sample similar cosmological volumes (i.e., similar redshift distributions). L[O III] is consistently a trait that distinguishes the mega-masers from the non-masers (control), as in Zhu et al. (2011).

K-S Statistics for Maser/Non-maser Parameter Comparisons

Variable	Masers/Control	Maser/Megamasers	Control/Megamasers
z	0.72	0.91	0.91
Log(SFR)	0.0018	0.85	$< 1 \times 10^{-4}$
Log L[OIII]	$< 1 \times 10^{-4}$	1.00	$< 1 \times 10^{-4}$
Log L[OI]	0.00065	0.98	$< 1 \times 10^{-4}$
S[II] Ratio	0.091	0.91	0.00030
Hα/Hβ	0.52	0.43	$< 1 \times 10^{-4}$
σ^*	0.0026	0.73	$< 1 \times 10^{-4}$
L/L_{edd}	0.10	0.90	$< 1 \times 10^{-4}$

The comparisons of overall distributions of a variety of optical host and nuclear properties of maser and non-maser galaxies support previous findings of, e.g., Zhu et al. (2011) that maser galaxies show statistically higher levels of reddening and extinction, i.e., higher Balmer decrements & that maser galaxies are more massive (higher stellar mass M*), more luminous (in M_r, not shown here), and harbor more massive BHs in their centers (as shown by the comparison in σ*).

Nevertheless, our analysis reveals new findings:

1. Galaxies with very massive BHs (σ* > 200 km/s) do not host masers; physical conditions in the vicinity of such systems may not be stable enough to sustain strong mega-maser, or especially disk maser emission.
2. There is a potential "goldilocks range" in quite a few maser galaxy parameters:

i) n_e spans only a range of ~100–300 cm^3 (corresponding to [S II] λ 6716/λ6731 = 1.4 – 1);
ii) both M_{BH} and L/L_{Edd} are narrowly centered on what appears to correspond to a change in the accretion flow geometry or mode, from efficient (i.e., Shakura-Sunyaev standard accretion disk/corona, or quasar-like, Shakura & Syunyaev 1973) to inefficient (i.e., the radiatively inefficient, or advection dominated accretion flow; RIAF/ADAF; e.g., Narayan & Yi 1994) with decreasing L/Ledd (e.g., Constantin et al. 2009).
This may suggest that the **disk mega-maser emission is related to a certain (short) phase in the galaxy-AGN evolution**, reflected in this particular change.

Correlations Among Properties

support differences seen in overall distributions between maser disks, mega-masers, masers in general and non-maser galaxies.

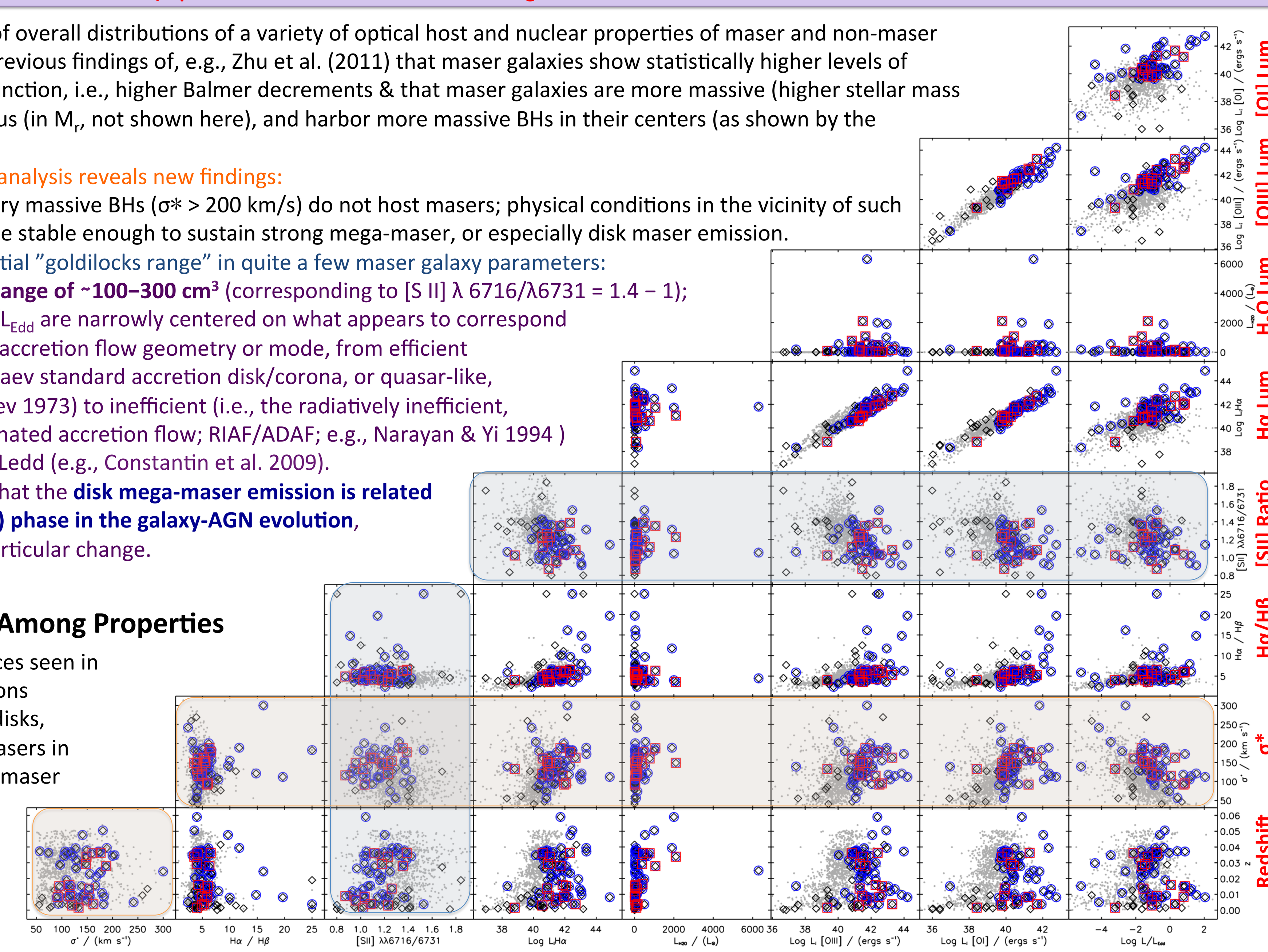

Principal Component Analysis (PCA)

PCA is a dimension reduction technique that eliminates any redundancies in the data. This idea is demonstrated to the right: by analytically picking appropriate linear combinations of parameters we can create a more accurate measure of the variability in a data set. The PCA is an exploratory analysis in that it reveals otherwise hidden trends and correlations.

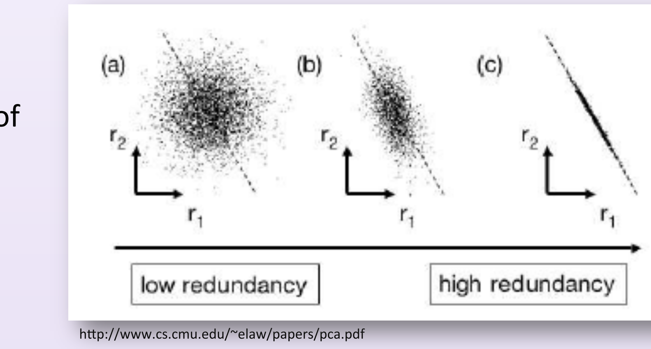

Eigenvectors for combined masers and control

Variable	EV-1 31.6%	EV-2 47.2%	EV-3 59.0%	EV-4 69.4%	EV-5 78.2%
z	0.218	**-0.448**	-0.164	-0.404	-0.320
σ^*	0.276	0.182	0.254	-0.008	0.062
Hα/Hβ	0.002	0.111	**0.664**	-0.238	-0.625
λλ6716/6731	-0.090	0.146	-0.357	-0.792	0.043
Log L [OIII]	0.275	**-0.620**	0.025	0.021	-0.012
Log [OIII]/Hβ	**0.389**	-0.337	-0.001	0.147	0.044
Log [NII]/Hα	**0.450**	0.282	0.057	-0.022	-0.083
Log [SII]/Hα	**0.442**	0.309	-0.178	-0.037	0.034
Log [OI]/Hα	**0.489**	0.217	-0.119	0.013	0.036
L H_2O	0.070	-0.113	**0.540**	-0.358	0.700

PCA statistics of the combined maser and control samples: The eigenvectors are linear combinations of the parameters shown and each corresponding value is the weight of the parameter. Values in **bold** indicate significant correlations. EV1 confirms that the spectral type (as defined by the 4 flux ratios) is the most significant contributor to the variance in the data, consistent to what the BPT diagram shows. EV2 is dominated by the correlation of redshift z and L[OIII], generally expected for any sample. EV3 is dominated by the correlation of the Hα/Hβ and the maser luminosity L(H_2O), suggesting that the maser activity depends on the obscuration of the nuclear region.

Plots of EV1 vs. the line ratios employed in optical classifications show that the masers, and especially the mega-masers or the disks, are well clustered within a certain parameter space. This indicates that the mega-masers are indeed quantifiably different from the non-masers. Various PCA tests for sets of measures separated by maser/non-maser based on a priori known correlations among parameters show significantly different weights, supporting a dissimilarity in properties between maser and non-maser systems.

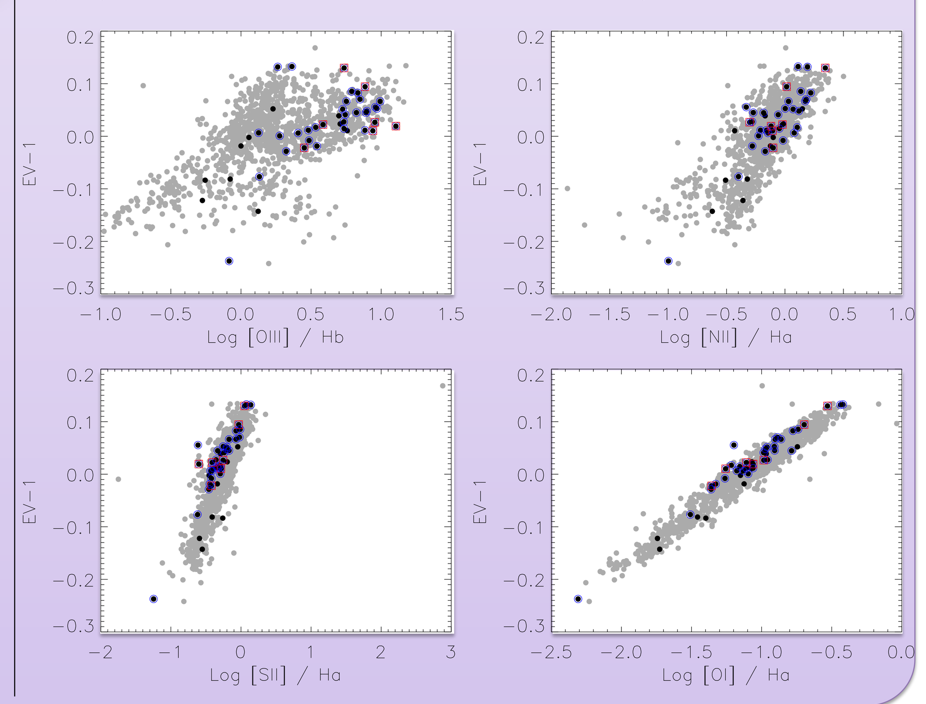

Discriminant Analysis (DA)

DA is a multidimensional statistical analysis similar to PCA, with the important distinction that it is predictive and not exploratory. DA maximizes the separation of two or more groups in their variable space, and provide a quantitative combination of parameters that contribute the most to this separation. In our case the two groups are the non-masers and the masers (or mega-masers or disks) and the variables are the optical spectral and photometric data. The table above shows the performance of the analysis on our known masers and non-masers (i.e. the training set); the predictions and their associated errors represent the optimistic maximum. The model based on the training set can then be applied to any other object with the same set of measurements. We are currently doing this to a set of 300,000 galaxies from the MPA-JHU SDSS DR7 spectroscopic data catalogue (see table for preliminary results), and will test the proposed target set with future observations at Green Bank Telescope.

Table of Discriminant Analysis Predictions

Type	Maser			Mega-Maser			Disk		
	Masers	Control	% of Total Masers	Masers	Control	% of Total Masers	Masers	Control	% of Total Masers
Total	1735	298851	100%	1191	299395	100%	888	299698	100%
HII	1088	210881	63%	573	211396	48%	612	211357	69%
Transition	126	52848	7%	113	52861	9%	16	52958	2%
Seyfert	389	12142	22%	383	12148	32%	238	12293	27%
LINER	129	22978	7%	119	22988	10%	21	23086	2%

Constraining The Detection Rate

Because of its multidimensionality, the DA is more of a numerical tool than a visual aid, so here is a visual example of how a 2-parameter constraint can increase the mega-maser detection rate by a factor of ~3. Suppose the survey for mega-masers is conducted only for galaxies with a [S II] ratio between 1 and 1.4, and an [O III] luminosity >~ 10^{40} ergs/s, the detection rate jumps from <3% outside the region to 14% inside the region. This is essentially what the DA does but for the entire N-parameter space.

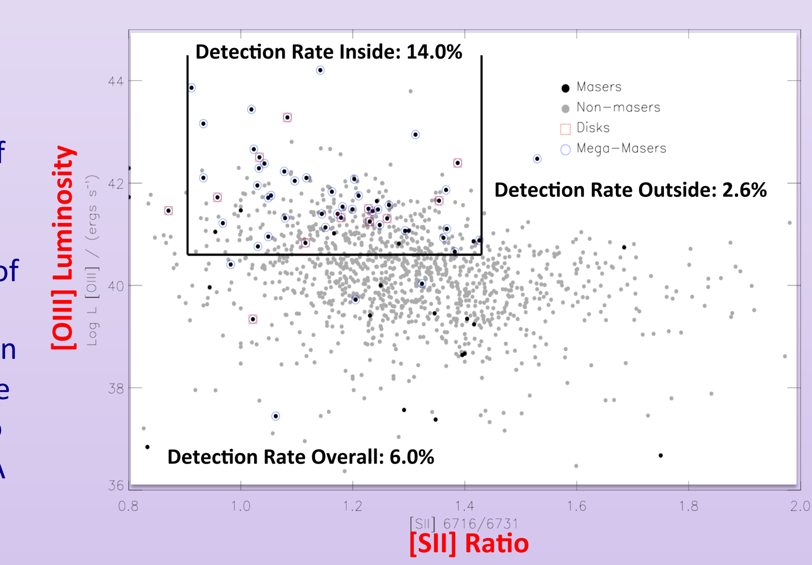

Adams, T. F., & Weedman, D. W. 1975, ApJ, **199**, 19
Bennert, N., Schulz, H., & Henkel, C. 2004, A&A, **419**, 127
Braatz, J. A., Reid, M. J., Humphreys, E. M. L., Henkel, C., Condon, J. J., & Lo, K. Y., 2010, ApJ, **718**, 657
Brinchmann, J., Charlot, S., Heckman, T. M., Kauffmann, G., Tremonti, C., & White, S. D. M. 2004, arXiv:astro-ph/0406220
Buttiglione, S., Capetti, A., Celotti, A., et al. 2009, A&A, **495**, 1033
Constantin et al., 2009, ApJ, **705** 1336
Dahari, O., & De Robertis, M. M. 1988, ApJS, **67**, 249
De Robertis, M. M., & Osterbrock, D. E., 1986, ApJ, **301**, 98
Goodrich, R. W., & Osterbrock, D. E. 1983, ApJ, **269**, 416
Ho, L., Fillippenko, A., Sargent, W., 1997, ApJS **112**, 315
Kauffmann, G., et al. 2003, MNRAS, **341**, 33
Kauffmann, G., et al. 2004, MNRAS, **353**, 713
Kewley, L.J., Groves, B., Kauffmann, G., & Heckman, T., 2006, MNRAS, **372**, 961
Kim, D. C., Sanders, D. B., Veilleux, S., Mazzarella, J. M., & Soifer, B. T. 1995, ApJS, **98,** 129
Miyoshi, M., Moran J.M., Herrnstein J., Greenhill L., Nakai N., et al.1995, Nature, **373**, 127
Moustakas, J., & Kennicutt, Jr., R. C. 2006, ApJS, **164**, 81
Narayan, R., & Yi, I., 1994, ApJ, **428**, 13
Neugebauer, G., Becklin, E. E., Oke, J. B., & Searle, L. 1976, ApJ, **205**, 29
Osterbrock, D. E., & De Robertis, M. M. 1985, PASP, **97**, 1129
Phillips, M. M., Charles, P. A., & Baldwin, J. A., 1983, ApJ, **266**, 485
Reid, M. J., Braatz, J. A., Condon, J. J., Greenhill, L. J., Henkel, C., & Lo, K. Y. 2009, ApJ, **695**, 287
Shakura, N. I., & Syunyaev, R. A. 1973, A&A, **24**, 337
Whittle, M. 1992, ApJS, **79**, 49
Zhu, G., Zaw, I., Blanton, M. R., & Greenhill, L. J., 2011, ApJ, **742**, 73